Article:
Baraldi, D, Milani, G and Sarhosis, V orcid.org/0000-0002-8604-8659 (2021) A Rigid-Beam-Model for studying the dynamic behaviour of cantilever masonry walls. Structures, 33. pp. 2950-2963. ISSN 2352-0124

https://doi.org/10.1016/j.istruc.2021.05.095

A Rigid-Beam-Model for studying the dynamic behaviour of cantilever masonry walls

Daniele Baraldi[1], Gabriele Milani[2], and Vasilis Sarhosis[3]

[1] Università IUAV di Venezia
Terese, Dorsoduro 2206, 30123, Venice, Italy
e-mail: danielebaraldi@iuav.it

[2] Technical University of Milan, Department of Architecture, Built Environment and Construction Engineering
Piazza Leonardo Da Vinci 32, 20133, Milano, Italy
gabriele.milani@polimi.it

[3] University of Leeds, School of Civil Engineering
LS2 9JT, Leeds, UK
V.Sarhosis@leeds.ac.uk

Abstract

In this work, a simple and effective Rigid Beam Model recently introduced for studying the dynamic behaviour of ancient freestanding stone columns is extended to the case of cantilever unreinforced masonry walls, considered along their thickness and subjected to out-of-plane loading. Both monolithic and multi-block walls were investigated. The proposed model assumes each block of the wall as a rigid beam element and each interface as a node. By assuming no sliding along the interfaces and small displacements of blocks, rocking can be simulated by a bi or tri-linear moment rotation non-linear constitutive law. Different in geometry monolithic and multi-block masonry walls were developed in the numerical model and subjected to different in magnitude and frequency harmonic loading. Their response was compared against those from the literature and good agreement was found. From the analysis results, it was found that monolithic walls can overturn with acceleration magnitudes larger than their corresponding static load multipliers, if input frequency values increase. However, overturning accelerations of multi-block walls increase less rapidly for increasing input frequency with respect to the corresponding equivalent monolithic walls. Collapse mechanisms involving wall portions above the base were found in addition to traditional overturning ones with respect to the base. To ensure reproducibility of results, input and output files will be made publicly available.

Keywords: cantilever walls, masonry, out of plane response, dynamic loading

*Corresponding author: Daniele Baraldi, Università IUAV di Venezia, Terese, Dorsoduro 2206, 30123, Venice, Italy, e-mail: danielebaraldi@iuav.it

1 INTRODUCTION

There are several buildings with primary structural wall systems of unreinforced masonry walls which have suffered damage from past earthquakes [**1**-**8**]. Potential collapse of such walls possesses a significant threat to anyone that would be next to the wall at the time of earthquake. It is well known that in-plane wall failures, if occur, will reduce the lateral load capacity of the walls. However, out-of-plane wall failures can result in collapse of the wall, which could lead in some cases to partial or total collapse of the building. It is often the case that out-of-plane wall failures occur due to inadequate anchorage of the wall to the floor diaphragms. When there is no anchorage of the wall to the diaphragm, the wall behaves as cantilever. In this case, collapse of the wall occurs when the

magnitude of inertial forces on the wall are such that stability of the wall is lost. However, when anchorage of the wall to the diaphragm exists, then the wall will behave as vertical beams in bending, since inertial forces will be distributed to the diaphragms. Now, since unreinforced masonry walls are characterized by limited strength at the mortar joints, when subjected to out of plane loading, they will crack at the bed joints and often just above the mid-height of the wall. In this case, the top and bottom wall segments will rock in the out of plane direction. If the magnitude of displacement induced by the seismic motion is large, the wall can become unstable and eventually collapse. Also, it is expected that walls at top storey are the most vulnerable to failure as they are withstanding lower axial loads.

From the above, understanding of out-of-plane response of masonry walls is essential for the structural assessment and vulnerability of existing buildings and the investigation of this problem represents an extremely active field of research in the structural engineering field. For instance, a literature review related to masonry out-of-plane behaviour and to the corresponding numerical models was done by Ferreira et al. [**9**], and more recently by Sorrentino et al. [**10**] by also focusing on several national design codes, whereas a more general deep review on different modelling strategies for masonry was done by D'Altri et al. [**11**]. As well known, the out of plane behaviour of masonry panels is governed by many parameters, such as boundary conditions, constraint quality, blocks arrangement, materials, loads, geometry, and slenderness. Many contributions dealing with these aspects and involving different numerical strategies can be found in literature [**12**-**33**].

Many experimental tests have been performed up to recent years [**34**-**41**] for assessing the out-of-plane behaviour of masonry walls. Several tests characterized by strong ground motions applied by shaking tables demonstrated that given sufficient anchorage to the diaphragms, unreinforced masonry walls subjected to out of plane actions can maintain stability [**34**-**39**]. In particular, Gulkan et al. [**34**] tested single storey masonry houses and found large displacements when the out of plane walls rocked at mid-height crack without collapse. However, when the structure subjected to in-plane and out of plane ground motions, the out of plane response of walls did not increase. Moreover, Griffith et al. [**37**] found that the magnitude of ground motion significantly affects the out of plane rocking response of the wall. Ground motions with low peak ground demand would damage the wall specimens. However, walls subjected to high peak ground demand resulted in rocking beyond the stability limit and collapse.
It is worth remembering that the first and probably the largest laboratory experimental campaign on walls subjected to out-of-plane dynamic excitation is that performed by the Agbabian–Barnes–Kariotis (ABK) consortium [**42**].

Freestanding walls can be considered in some cases as single rigid block structures resting on ground. Focusing on the analytical and numerical assessment of the dynamic performance of freestanding walls, many authors suggested several approaches in the last decades. The first scientific considerations on rigid bodies overturning due to seismic actions were carried out by Milne [**43**] and Omori [**44**]. However, the most important contribution in this field was proposed by Housner [**45**], who analytically investigated the behavior of moderately slender rigid bodies subjected to horizontal excitations, in order to estimate the minimum horizontal acceleration at the base causing the overturning of the system. This problem was then studied up to recent years by means of analytical, numerical and laboratory experimentations [**46**-**58**]. In particular, the rocking response of blocks subjected to harmonic loading was studied by Spanos and Koh [**50**], that identified 'safe' and 'unsafe' regions depending on acceleration and frequency of the excitation. Their study was extended by Hogan [**59**,**60**]. Research on walls considered as monolithic ones by means single-degrees-of-freedom (SDOF) models subjected to dynamic loading was carried out also by Doherty, Griffith, Lam and co-workers [**61**-**64**], Sorrentino et al. [**65**]. However, SDOF models are able to predict collapse mechanisms characterized by the overturning of the entire wall with respect to its support, whereas

models having at least two aligned rigid blocks can investigate potential collapse mechanisms involving the overturning of wall portions above the base.
Several research activities considered freestanding walls composed of a small number of vertically aligned rigid blocks [**66**-**70**], which were able to simulate the rocking of a block with respect to another one [**68**]. However, these cases often do not realistically represent the behavior of a masonry wall made of natural or artificial blocks.
Considering multi rigid block, or multi-degree of freedom (MDOF), structures, several authors [**71**-**76**] have successfully used the discrete element method (DEM) to study the rocking motion of freestanding walls. However, most of the contribution in this field, even if performed in a two-dimensional framework, are mainly focused on simulating the behaviour of freestanding columns, rather than masonry walls [**77**-**81**].
The importance of using multi-block models was effectively highlighted by D'Ayala and Shi [**82**]. Observing experimental tests, they stated that single blocks can move at the top level and that walls can be divided into portions with varying geometric ratios, rocking and sliding with respect to each other. In some cases, the bottom portion of the wall does not move and remains rigidly jointed to the base.
A recent literature review dedicated to both SDOF and MDOF models for studying out-of-plane wall behavior was proposed by Casapulla et al. [**83**].

Now, with respect to international standards and codes used for the seismic assessment of the out of plane failure mechanism of existing unreinforced masonry walls, these involve force-based and displacement-based methods. The two methods are based on the static analysis and make use of the kinematic approach of limit analysis. The force-based method can be used to predict the acceleration that leads the wall to collapse by means of the force capacity of the wall and the behavior factor q. The displacement-based method considers the entire force-displacement behavior of the wall and predicts the acceleration that leads the wall to collapse by comparing its displacement capacity with displacement demand [**85**]. The Italian standards [**86**] are the only code which considers both force-based and displacement-based methods. Moreover, the seismic vulnerability standards addressed by ASCE/SEI 41 [**84**], specifies acceptable collapse prevention criteria based on the height-to-thickness ratio for out of plane walls with sufficient anchorage to the diaphragms. Such limits are related to the spectral acceleration (S_a) for a period of 1.0s. Such provisions were based on an experimental test of 22 wall specimens with varying height-to-thickness ratios subjected to dynamic loading at both top and bottom and undertaken by ABK joint venture [**42**].

The performance of force-based and displacement-based seismic assessment methods for evaluating the out of plane behavior of unreinforced masonry walls evaluated on the bases of refined numerical models. In the study of Godio and Beyer [**87**], a DEM of a vertically spanning wall was developed and validated against experimental finding. The numerical model was based on the commercial code Itasca [**88**] developed by Cundall [**89**]. A large range of wall with different dimensions were analysed. Both static pushover analysis and incremental dynamic ones were undertaken to determine the capacity of the wall. It was found that the displacement-based method is more accurate, robust, and safer than the force-based method. In addition, walls characterised by a relatively high ratio of axial load to Euler's critical load, both assessment methods lead to an overestimation of the wall capacity. A year later, a trilinear model describing the force-displacement response of vertically spanning unreinforced masonry walls was investigated by Godio and Beyer [**90**]. The various factors influencing the response of the walls (e.g. the support conditions, the level of applied axial load, the slenderness ratio, and the deformability of the wall) were investigated. The model was validated against experimental results from shake table tests while the force and displacement parameters of the model were described by analytical expressions. Al Shawa et al. [**58**] compared the force-based and displacement-based methods against results obtained from shake table tests and from non-linear time history analyses developed by numerical and analytical models. Pre-damaged URM walls

subjected to out of plane ground motions and undergoing rocking were undertaken; the numerical model consisted in a discrete element model in which the wall was idealized as a single rigid block. The analytical model used the force based and displacement-based assessment using a single degree of freedom system with a trilinear force-displacement relationship. Both numerical and analytical models were calibrated on the tested configurations and then used to perform a sensitivity study. The force-based and the displacement-based assessment methods undertaken in [**58**] were found to be conservative by 99% and 90% of the cases, respectively. The study was extended by Sorrentino et al [**10**] in which a single degree of freedom with trilinear force-displacement relationship was used to study free standing cantilever walls as well as walls spanning vertically between two supports. From the analysis results, it was found that the displacement-based method yielded less scattered results with respect to the force-based method and, for this reason, it was considered more efficient in predicting the peak dynamic response of the walls.

In order to suggest a new simple and efficient approach to understand and simulate the behavior of freestanding masonry walls out-of-plane loaded, a Rigid Beam Model, already introduced by authors for studying the dynamic behavior of monolithic and multi-drum freestanding columns [**91**], is here extended for representing freestanding walls subjected to out-of-plane dynamic actions. The model is introduced in plane state conditions, hence by considering the transversal section of the wall, whereas the blocks arrangement along wall depth is not taken into consideration. Monolithic or multi-block walls are investigated, in the latter case by assuming equally-spaced wall portions in vertical direction, which may represent on one hand actual stone, clay or concrete blocks connected by mortar joints, on the other hand they can represent portions of wall made of irregular stones, where the interfaces may represent potential horizontal cracks. The rigid beam model assumes each block or wall portion as a rigid beam element and each interface between the blocks as a node of the model. Small displacements hypothesis is introduced and no sliding at the interfaces is considered; then, model displacements are given by block rigid rotations and the nonlinear behavior of the system is lumped at interface or nodal level, by accounting for the potential rocking between the blocks by means of bi- or tri-linear moment-rotation constitutive laws. An infinite compressive strength and a negligible tensile strength is also assumed at interface level. The no-sliding turns out to be more appropriate for masonry walls instead of freestanding ancient columns, originally considered for introducing the model.

A set of numerical tests is performed by applying harmonic accelerations at the base of monolithic and multi-block cantilever walls, by varying input frequency and acceleration magnitude, and by considering several case studies having different wall slenderness. The term ‘cantilever’ is used for describing a freestanding wall connected to a base foundation and free to move at its top. The manuscript is organized as follows. The rigid beam model for cantilever walls is introduced by highlighting the hypotheses adopted for its definition and by describing its kinematics; then, the equations of motion of the model are presented and the corresponding matrix representation is highlighted, together with the nonlinear behavior considered at interface level. The numerical tests are then presented, starting with thick monolithic walls, considering slender monolithic walls, and ending with a more realistic case study represented by a multi-block wall made of hollow concrete blocks. The last case study is further investigated by performing a sensitivity analysis varying several geometrical parameters of the model, in order to highlight different types of overturning collapse mechanisms that may arise during the dynamic tests, in agreement with the considerations of D’Ayala and Shi [**82**].
Finally, some comments on model simplicity and effectiveness are done, together with some considerations on possible further developments and improvements of the current version of the model.

2 RIGID BEAM MODEL FOR CANTILEVER WALLS

In this work, a freestanding or cantilever unreinforced masonry wall (or parapet) subjected to out-of-plane actions is considered. The wall is resting on a rigid foundation, without side supports and free to move at its top. This wall typology is probably the most vulnerable to overturning out-of-plane failure mechanisms (Fig. 1a), as shown by the pioneering considerations done by Rondelet [**92**]. Considering the vertical cross-section of the freestanding wall, it can be subdivided into n layers of blocks or wall portions. Interfaces between the layers or portions can represent the actual horizontal joints of a regular texture of blocks connected by dry or mortar joints (Fig. 1b,c), in case of a well-built masonry wall made of prismatic blocks, or they can represent potential horizontal cracks into a wall made of irregular stones (Fig. 1d).

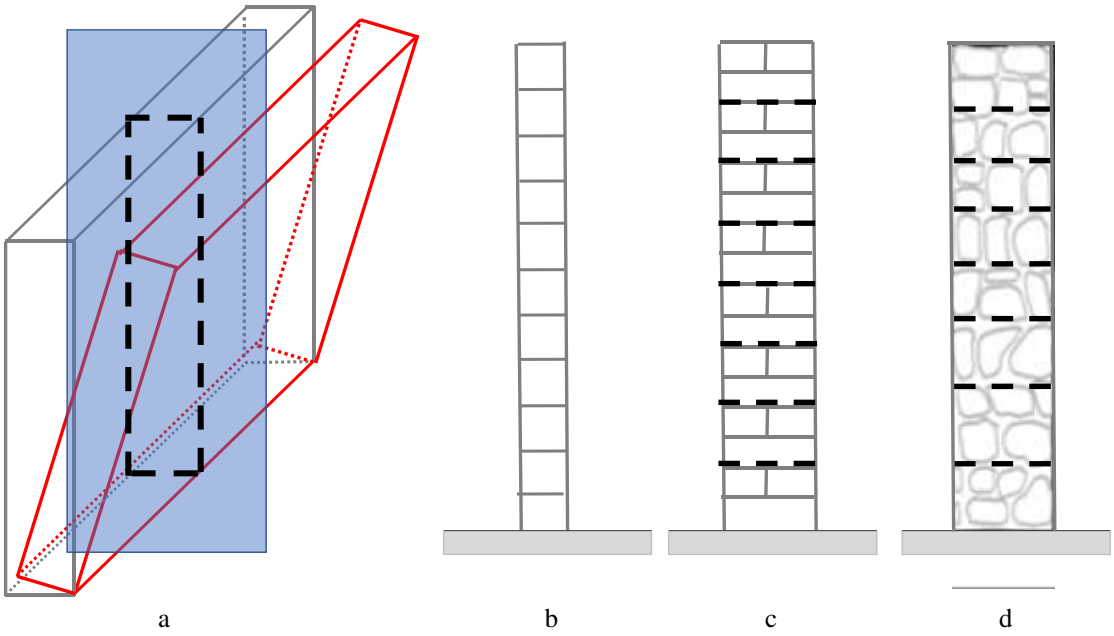

Figure 1: Freestanding masonry wall subjected to an overturning collapse (a); vertical sections of multi-block freestanding/cantilever walls derived from a one-headed masonry wall (a), a two-headed masonry wall (b), and from a wall made of irregular stones (b).

The wall has an overall height H and the block layers or wall portions, at this stage of the research, are assumed to be equally spaced, hence $h_i = H/n$ is the height of the generic i-th block or wall portion. A two-dimensional coordinate system Oxy is introduced, since analyses are performed in plane state, accounting for a uniform wall depth along its height. Wall thickness is defined by B and it is assumed to be uniform along wall height (Fig. 2a); however, the model is also able to consider a linearly variable thickness of the wall, hence the dimensions B_1 and B_2 are equal to the width of the lower cross-sections at the base and at the top of the wall, respectively (Fig. 2b). As it will be underlined in the final section of this contribution, the proposed model can be easily improved for considering walls composed by block layers having different height; furthermore, different thickness values along wall height can be taken into consideration, in order to simulate, for instance, the behaviour of an entire multi-storey masonry façade with a small thickness at the top level and a large thickness at the foundation level.

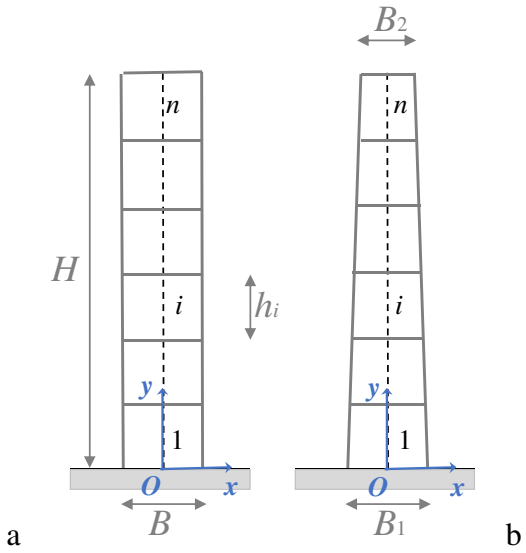

Figure 2: 2D model for a multi-block cantilever wall having uniform width along its height (a) and linearly varying width along its height (b).

2.1 Model hypothesis and kinematics

The rigid beam model is introduced by defining n rigid beam elements and $n + 1$ nodes at the ends of the beam elements as shown in Fig. 3a, b. Each beam element represents a block or a uniform wall portion and each intermediate node between the beam elements represents an interface or a joint between the blocks or wall portions. In particular, the first node represents the contact interface between the ground and the first block, whereas the last node represents the tip of the wall. In case of wall thickness linearly varying along its height, the cross-section of each beam element is assumed to be constant, hence each wall portion has an average cross section width d_i, leading to a stacked rigid block wall.

The kinematics of the model is defined by horizontal nodal translations, velocities, and accelerations u_i, $\dot{u}_i = du_i / dt$, and $\ddot{u}_i = d^2u_i / dt^2$, respectively. Small displacements hypothesis is assumed, hence, together with to the rigid beam hypothesis, vertical translations of the nodes are neglected, and the rigid rotation of the generic beam element can be defined as function of the corresponding upper and lower horizontal translations and beam element height:

$$\theta_i = \frac{u_{i+1} - u_i}{h_i} \tag{1}$$

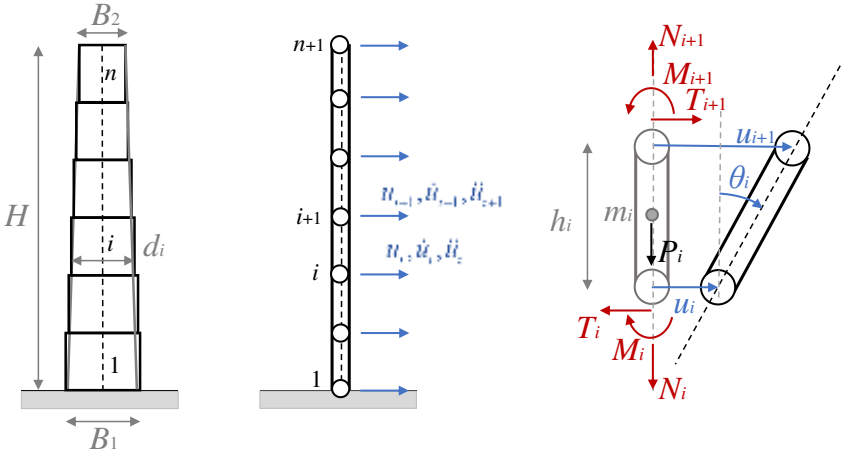

a b c

Figure 3: Multi-block (stacked) cantilever wall (a), corresponding rigid beam model (b), generic beam element (c).

The potential sliding between the wall portions is neglected by the proposed model, whereas the relative rotations between the wall portions and the consequent rocking are taken into consideration. This hypothesis turns out to be more suitable for masonry walls instead of ancient columns originally considered for introducing the rigid beam model. At this stage of model development, interfaces between the portions have an infinite compressive strength and a negligible tensile strength.

2.2 Equations of motion

Each *i*-th beam element is characterized by a mass m_i, which is equal to the mass of the corresponding block or wall portion. Internal forces of the beam elements are given by a shear force T_i, and a bending moment M_i, acting at each *i*-th node of the model (Fig. 2c); a normal force N_i is also present due to wall self-weight. At this stage of development of the model, no further vertical loads are considered. The translational equation of motion in horizontal direction and the rotational equation of motion for the generic *i*-th beam element may be written as follows:

$$\begin{aligned} \frac{\ddot{u}_{i+1} + \ddot{u}_i}{2} m_i &= T_{i+1} - T_i \\ \ddot{\theta}_i I_{G,i} &= -M_{i+1} + M_i + T_{i+1}\frac{h_i}{2} + T_i \frac{h_i}{2} \end{aligned} \qquad (2a,b)$$

And the equilibrium in vertical direction is given by:

$$P_i = V_i \cdot \gamma \cdot g = N_{i+1} - N_i \qquad (3)$$

where $i = 1, \ldots, n+1$, P_i is the weight of the generic block, depending on block volume V_i and material density γ, and $I_{G,i}$ is its polar inertia.

2.2.1 – Translational equations of motion

Considering a freestanding wall subjected to a horizontal ground acceleration $a_g(t)$, equations of motion (2a,b) have to follow the subsequent boundary conditions at wall base (1st node) and wall top (n+1 node):

$$\begin{aligned} \ddot{u}_1 &= \ddot{u}_g = a_g(t) \\ T_{n+1} &= 0 \\ M_{n+1} &= 0 \end{aligned} \qquad (4a,b,c)$$

According to such conditions, the translational equations of motion (Eq. 2a) for the last and penultimate (n-th and n-1-th) beam elements turn out to be:

$$\begin{aligned} \frac{\ddot{u}_{n+1} + \ddot{u}_n}{2} m_n &= -T_n \\ \frac{\ddot{u}_n + \ddot{u}_{n-1}}{2} m_{n-1} &= T_n - T_{n-1} \end{aligned} \qquad (5a,b)$$

Substituting the 1st of the previous equations into the 2nd one, the following expression is obtained:

$$T_{n-1} = T_n - \frac{\ddot{u}_n + \ddot{u}_{n-1}}{2} m_{n-1} = -\frac{\ddot{u}_{n+1} + \ddot{u}_n}{2} m_n - \frac{\ddot{u}_n + \ddot{u}_{n-1}}{2} m_{n-1} =$$
$$= -\frac{1}{2}[\ddot{u}_{n+1} m_n + \ddot{u}_n (m_n + m_{n-1}) + \ddot{u}_{n-1} m_{n-1}] \tag{6}$$

More generally, the shear force acting at the generic *i*-th node of the rigid beam model can be written as function of the nodal accelerations of nodes from *i* to *n*+1 and of the masses of the beam elements from *i* to *n*. In particular, the translational equation of motion for the 1st beam element is given by:

$$\frac{\ddot{u}_2 + a_g(t)}{2} m_1 = T_2 - T_1$$
$$T_1 = T_2 - \frac{\ddot{u}_2 + a_g(t)}{2} m_1 \tag{7a,b}$$

where T_1 turns out to depend on the nodal accelerations and masses of the whole rigid beam model. Hence, the translational equations of motion of the entire rigid beam model can be written in matrix extended form as follows:

$$\begin{bmatrix} T_1 \\ T_2 \\ .. \\ T_{n-1} \\ T_n \end{bmatrix} = -\frac{1}{2} \begin{bmatrix} m_1 & m_1 + m_2 & .. & m_{n-2} + m_{n-1} & m_{n-1} + m_n & m_n \\ 0 & m_2 & .. & m_{n-2} + m_{n-1} & m_{n-1} + m_n & m_n \\ .. & .. & .. & .. & .. & .. \\ 0 & 0 & .. & m_{n-1} & m_{n-1} + m_n & m_n \\ 0 & 0 & .. & 0 & m_n & m_n \end{bmatrix} \begin{bmatrix} \ddot{u}_2 \\ \ddot{u}_3 \\ .. \\ \ddot{u}_n \\ \ddot{u}_{n+1} \end{bmatrix} - \frac{1}{2} \begin{bmatrix} a_g(t) m_1 \\ 0 \\ .. \\ 0 \\ 0 \end{bmatrix} \tag{8}$$

and in matrix compact form as follows:

$$\mathbf{t} = -\frac{1}{2}[\mathbf{M}\ddot{\mathbf{u}} + \mathbf{a}_g] \tag{9}$$

where the vector $\mathbf{t}$ collects the shear forces of the model $\mathbf{t} = [T_1\ T_2\ \ldots\ T_n]^T$, vector $\ddot{\mathbf{u}}$ collects horizontal accelerations from node 2 to *n*+1: $\ddot{\mathbf{u}} = [\ddot{u}_2\ \ddot{u}_3 \ldots \ddot{u}_{n+1}]^T$, and matrix $\mathbf{M}$ can be defined as a mass coefficient matrix of the multi-block wall.

2.2.2 – Rotational equations of motion

Following the approach adopted for the nodal shear forces and according to the boundary conditions, the rotational equations of motion (Eq. 2b) for the last and penultimate (*n*-th and *n*-1-th) beam elements turn out to be:

$$\ddot{\theta}_n I_{G,n} = M_n + T_n \frac{h_n}{2}$$
$$\ddot{\theta}_{n-1} I_{G,n-1} = -M_n + M_{n-1} + (T_n + T_{n-1}) \frac{h_{n-1}}{2} \tag{10a,b}$$

Where the height of the wall portions is detailed for each portion, but at this stage of model development it is always equal to *H*/*n*.

The equations above can be re-written by introducing the definition of block rotation (Eq. 1)

$$M_n = -T_n \frac{h_n}{2} + I_{G,n} \frac{\ddot{\theta}_{n+1} + \ddot{\theta}_n}{h_n}$$
$$M_{n-1} = M_n - (T_n + T_{n-1}) \frac{h_{n-1}}{2} + I_{G,n-1} \frac{\ddot{\theta}_n + \ddot{\theta}_{n-1}}{h_{n-1}} \qquad (11a,b)$$

Substituting the 1st of the equations above into the 2nd one, the following expression is obtained:

$$M_{n-1} = -T_n \frac{h_n}{2} - (T_n + T_{n-1}) \frac{h_{n-1}}{2} + I_{G,n} \frac{\ddot{\theta}_{n+1} + \ddot{\theta}_n}{h_n} + I_{G,n-1} \frac{\ddot{\theta}_n + \ddot{\theta}_{n-1}}{h_{n-1}} \qquad (12a,b)$$

More generally, the generic bending moment at the *i*-th node can be written as function of the nodal accelerations and shear forces of nodes from *i* to *n*+1, and of the polar inertia and height of the beam elements from *i* to *n*. In particular, the rotational equation of motion for the 1st beam element is given by:

$$\frac{\ddot{\theta}_2 - a_g(t)}{h_1} I_{G,1} = -M_2 + M_1 + (T_1 + T_2) \frac{h_1}{2}$$
$$M_1 = M_2 - (T_1 + T_2) \frac{h_1}{2} - \frac{\ddot{\theta}_2 - a_g(t)}{h_1} I_{G,1} \qquad (13a,b)$$

where M_1 turns out to depend on nodal accelerations, shear forces, polar inertias and drum height of the whole rigid beam model.
Hence, the rotational equations of motion of the entire rigid beam model can be written in matrix extended form as follows:

$$\begin{bmatrix} M_1 \\ M_2 \\ .. \\ M_{n-1} \\ M_n \end{bmatrix} = -\frac{1}{2} \begin{bmatrix} h_1 & h_1 + h_2 & .. & h_{n-2} + h_{n-1} & h_{n-1} + h_n \\ 0 & h_2 & .. & h_{n-2} + h_{n-1} & h_{n-1} + h_n \\ .. & .. & .. & .. & .. \\ 0 & 0 & .. & h_{n-1} & h_{n-1} + h_n \\ 0 & 0 & .. & 0 & h_n \end{bmatrix} \begin{bmatrix} T_1 \\ T_2 \\ .. \\ T_{n-1} \\ T_n \end{bmatrix} +$$
$$+ \begin{bmatrix} \frac{I_{G,1}}{h_1} - \frac{I_{G,2}}{h_2} & \frac{I_{G,2}}{h_2} & .. & \frac{I_{G,n-1}}{h_{n-1}} - \frac{I_{G,n}}{h_n} & \frac{I_{G,n}}{h_n} \\ -\frac{I_{G,2}}{h_2} & \frac{I_{G,2}}{h_2} - \frac{I_{G,3}}{h_3} & .. & \frac{I_{G,n-1}}{h_{n-1}} - \frac{I_{G,n}}{h_n} & \frac{I_{G,n}}{h_n} \\ .. & .. & .. & .. & .. \\ 0 & .. & -\frac{I_{G,n-1}}{h_{n-1}} & \frac{I_{G,n-1}}{h_{n-1}} - \frac{I_{G,n}}{h_n} & \frac{I_{G,n}}{h_n} \\ 0 & .. & 0 & -\frac{I_{G,n}}{h_n} & \frac{I_{G,n}}{h_n} \end{bmatrix} \begin{bmatrix} \ddot{\theta}_2 \\ \ddot{\theta}_3 \\ .. \\ \ddot{\theta}_n \\ \ddot{\theta}_{n+1} \end{bmatrix} - \begin{bmatrix} \frac{a_g(t) I_{G,1}}{h_1} \\ 0 \\ .. \\ 0 \\ 0 \end{bmatrix} \qquad (14)$$

And in matrix compact form as follows:

$$\mathbf{m} = -\frac{1}{2}\mathbf{H}\,\mathbf{t} + \mathbf{I}_G\ddot{\boldsymbol{\theta}} - \mathbf{b}_g \tag{15}$$

where vector **m** collects nodal bending moments from node *i* to *n*, $\mathbf{m} = [M_1\ M_2\ \ldots\ M_n]^T$, and vectors **t** and $\ddot{\boldsymbol{\theta}}$ have already been introduced with the translational equations of motion (Eq. 9). Matrices **H**, and $\mathbf{I}_G$ can be called, respectively, geometric coefficient matrix, and polar inertia coefficient matrix. Vector $\mathbf{b}_g$ is similar to $\mathbf{a}_g$ in Eq. 9, since it is characterized by null values except the first one, representing the rotational acceleration at the base of the column: $\mathbf{b}_g = [a_g(t) I_{G1} / h_1\ \ 0\ \ldots\ 0\ 0]^T$.

Substituting Eq. 9 into Eq. 15, the system of differential equations to be solved for obtaining the displacements of the masonry wall turns out to involve the nodal bending moments only, together with mass, inertia and geometric characteristics of the multi-block wall:

$$\mathbf{m} = \frac{1}{4}\mathbf{H}\,\mathbf{M}\,\ddot{\boldsymbol{\theta}} + \frac{1}{4}\mathbf{H}\,\mathbf{a}_g + \mathbf{I}_G\ddot{\boldsymbol{\theta}} - \mathbf{b}_g \tag{16}$$

Such a system of equations can be re-written in a more compact and simple form as follows:

$$\mathbf{m} = \left[\frac{1}{4}\mathbf{H}\,\mathbf{M} + \mathbf{I}_G\right]\ddot{\boldsymbol{\theta}} + a_g(t)\left[\frac{1}{4}\mathbf{H} - \frac{I_{G,1}}{h_1}\right]\mathbf{i} \tag{17}$$

where $\mathbf{i} = [1\ 0\ \ldots\ 0\ 0]^T$.

The system of differential equations above is solved by means of a Runge-Kutta ODE solver for stiff differential equations, low order method, by accounting for the nonlinear behavior of the interfaces between the blocks described in the upcoming sub-section.

2.3 Nonlinear behavior

Each bending moment M_i in **m** depends on the rotation θ_i of the corresponding *i*-th block (Eq. 1). Hence, Eq. 17 can be detailed as follows:

$$\mathbf{m}(\boldsymbol{\theta}) = \left[\frac{1}{4}\mathbf{H}\,\mathbf{M} + \mathbf{I}_G\right]\ddot{\boldsymbol{\theta}} + a_g(t)\left[\frac{1}{4}\mathbf{H} - \frac{I_{G,1}}{h_1}\right]\mathbf{i} \tag{18}$$

where $\boldsymbol{\theta} = [\theta_1\ \ \theta_2\ \ldots\ \theta_{n-1}\ \ \theta_n]^T$ collects block or wall portion rotations.

At this stage of development of the model, the nonlinear behavior that can affect the masonry wall is given by the rocking phenomenon at each interface between the blocks, whereas, following Housner's hypothesis [**45**], shear failure cannot occur, and sliding is neglected. The bending moment M_i at each interface follows a bilinear moment-rotation constitutive law, which defines the maximum stabilizing moment as function of block rotation (Fig. 4). The constitutive law adopted by the proposed rigid beam model is slightly modified with respect to Housner's law by means of an initial elastic stiffness $K_{M,i}$ instead of an infinitely rigid behavior, together with a smoothing parameter $\xi \leq 1$, which reduces the ultimate bending moment $M_{u,i}$, allowing to obtain a tri-linear law.

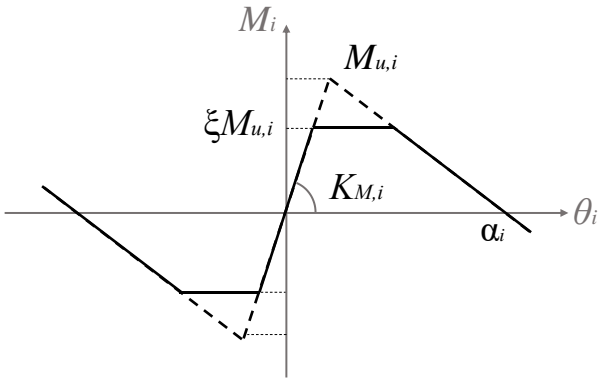

Figure 4: Moment-rotation relationship.

The maximum stabilizing moment in Fig. 3 is given by:

$$M_{u,i}\frac{d_i}{2}\sum_{j=i}^{n}P_j=\frac{d_i}{2}\sum_{j=i}^{n}m_j\cdot g=\frac{d_i}{2}\sum_{j=i}^{n}V_j\cdot\gamma\cdot g= \tag{19}$$

where d_i is the width of the i-th drum, hence $d_i/2$ represents the maximum eccentricity of the normal force admitted at the i-th joint, since an infinite compressive strength is assumed, together with no tensile strength at interface level. Interface bending stiffness $K_{M,i}$ depend on the elastic modulus of masonry E, on the moment of inertia of the interface I_i and on its thickness e_i, $K_{M,i} = E\ I_i\ /\ e_i$. The angle α_i represents the critical angle of the generic block [**45**], $\alpha_i = d_i/h_i$ in case of slender blocks.

3 DEVELOPMENT OF THE NUMERICAL MODELS AND RESULTS OBTAINED

The effectiveness the proposed Rigid Beam Model is evaluated by performing a set of numerical tests on monolithic and multi-block freestanding walls, by applying different simple ground excitations. For this purpose, several existing analytic and numerical results are taken into consideration in order to highlight differences and similarities of the proposed Rigid Beam Model with respect to existing formulations and numerical models. In particular, the numerical tests performed by Spanos and Koh [**50**] on simple rectangular monolithic walls subjected to harmonic excitations are reproduced and further parametric tests dedicated to wall slenderness are performed. Furthermore, the moderately slender monolithic wall studied in [**50**] is subdivided into equally spaced blocks or wall portions, in order to highlight the influence of potential rocking between the blocks in the dynamic behavior of the wall. Finally, a more realistic case study of a multi-block wall is considered by adopting a slender cantilever wall made of concrete hollow blocks subjected to harmonic excitations with varying input frequency and acceleration magnitude.

3.1 Monolithic walls

The analysis of monolithic walls may turn out to be generally more accurate with respect to multi-block walls due to the no-sliding hypothesis adopted by the proposed model, which may be ineffective in some conditions for representing the actual dynamic response of walls characterized by a large number of blocks, especially in case of dry joints between the blocks. However, many laboratory tests have demonstrated that well-built stone walls often behave as monolithic ones.

3.1.1 Thick and moderately slender monolithic walls subjected to harmonic excitation

The numerical tests performed by Spanos and Koh [**50**] on monolithic rectangular walls are considered. A thick and a moderately slender wall, having height to width ratio H/B equal to 2 and 4,

respectively, are subjected to harmonic excitations with varying input frequency and acceleration amplitude. Such specimens are here reproduced by means of the proposed Rigid Beam Model and considering a single rigid beam element. Harmonic excitations are applied for 10 seconds.
Starting with the thick wall case modelled with the proposed Rigid Beam Model, Figure 5 shows the deformed configurations at the end of the harmonic tests with several values of acceleration and frequency. The corresponding wall top and base displacements versus time are collected in Figure 6. Overturning conditions are obtained with 0.5g and 1Hz and with 1.0g with frequency values less than 1Hz.

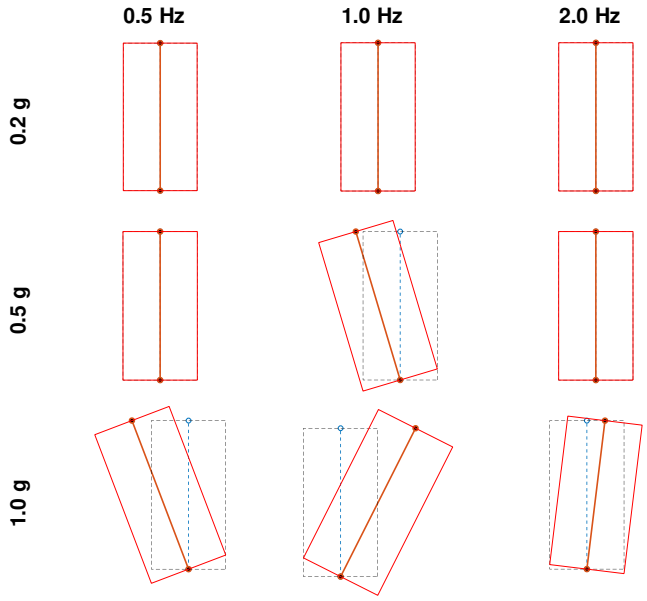

Figure 5: Deformed configurations for a thick monolithic wall ($H/B = 2$) subjected to several harmonic excitations

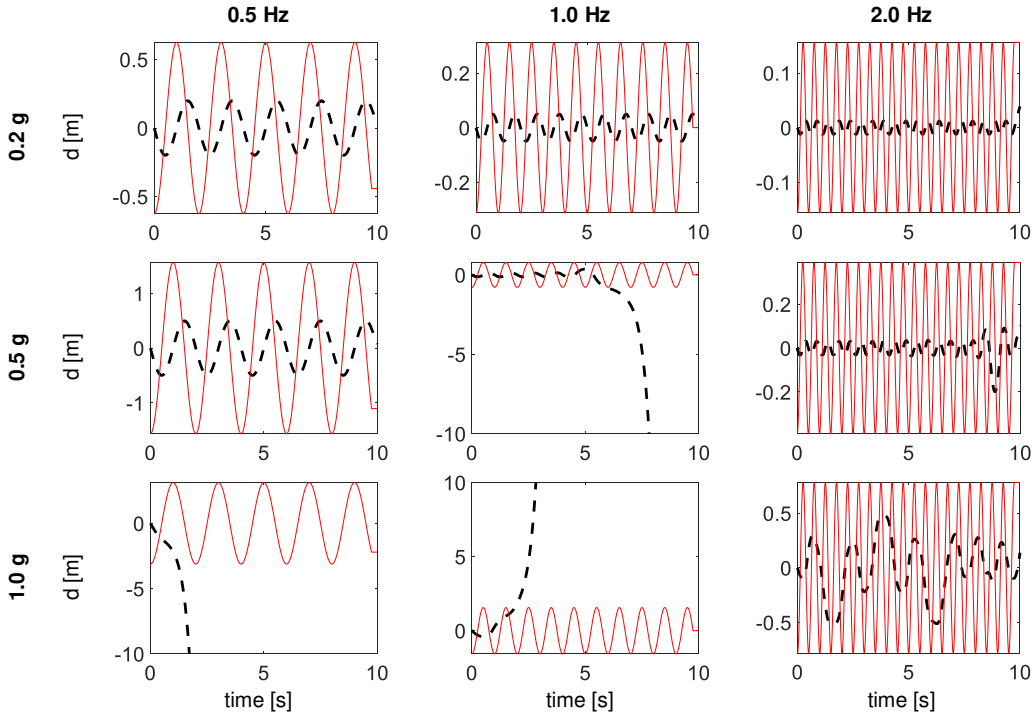

Figure 6: Base (red continuous line) and top (black dashed line) displacements for a thick monolithic wall ($H/B = 2$) subjected to several harmonic excitations

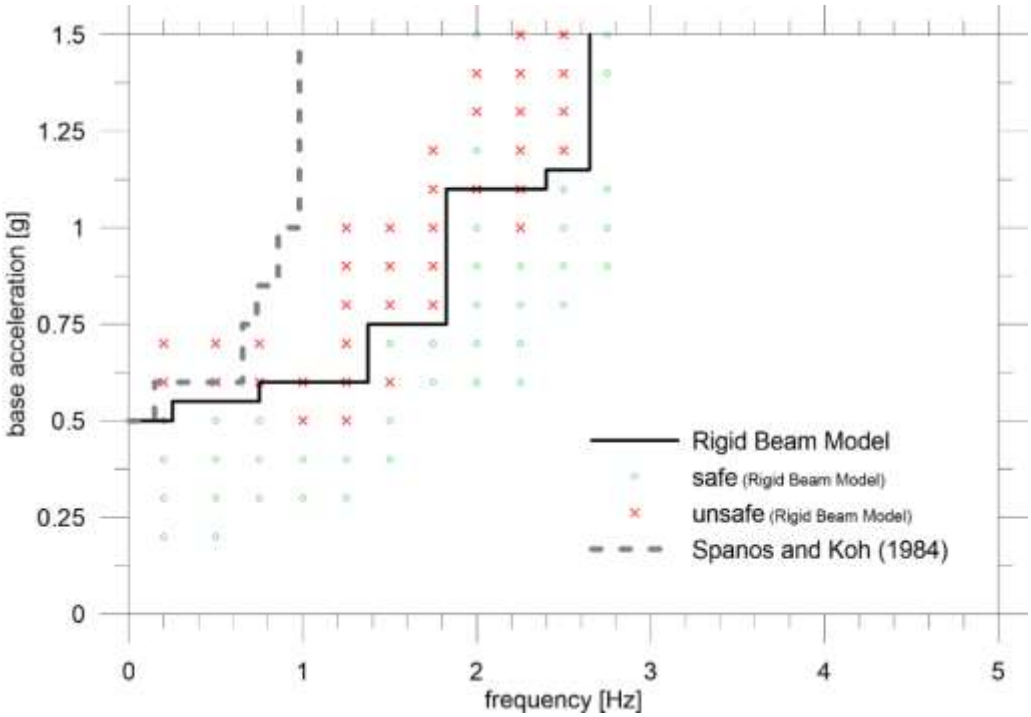

Figure 7: Safe-unsafe domain for a thick monolithic wall subjected to harmonic excitations

Figure 7 shows the safe-unsafe domain obtained with the Rigid Beam Model, which is significantly different with respect to that obtained in [**50**], probably due to the small H/B ratio of the case study considered and also due to the restitution factor close to 0.5 adopted in the reference work. In this case, both domains are characterized by a collapse acceleration equal to 0.5g for small frequency values, which is correctly coincident with the static collapse multiplier of the thick wall, namely $a_{g0} = (B/H)\ g = 0.5g$. For increasing frequency, the Rigid Beam Model allows to obtain overturning accelerations increasing to 1g with 2Hz and 1.5g close to 3Hz, whereas the collapse acceleration values obtained by Spanos and Koh increase rapidly to 1.5g close to 1Hz.
Focusing then on the moderately thick wall, Figure 8 shows several deformed configurations at the end of the numerical tests and Figure 9 collects base and top horizontal displacements versus time. Both the deformed configurations and the horizontal displacements at the top show overturning conditions obtained with 0.5g and 0.5Hz and 1Hz. More information about the possible overturning of the column are collected in Figure 10, which shows the safe-unsafe domain obtained with the Rigid Beam Model compared with that obtained in [**50**], who assumed in this case a restitution coefficient close to 1. Probably due to this condition, the two safe-unsafe-domains are in excellent agreement, both starting with a collapse acceleration equal to 0.25g, correctly corresponding to the static load multiplier for overturning the column, namely $a_{g0} = (B/H)\ g = 0.25g$, and with an increasing collapse acceleration for increasing frequency, up to 1.5g with 2Hz.

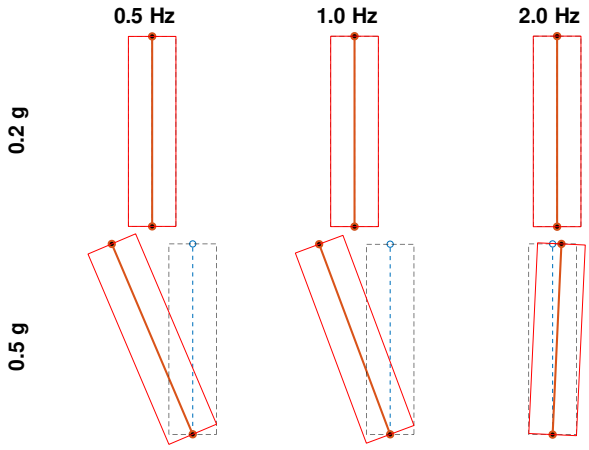

Figure 8: Deformed configurations for a moderately slender monolithic wall ($H/B = 4$) subjected to several harmonic excitations

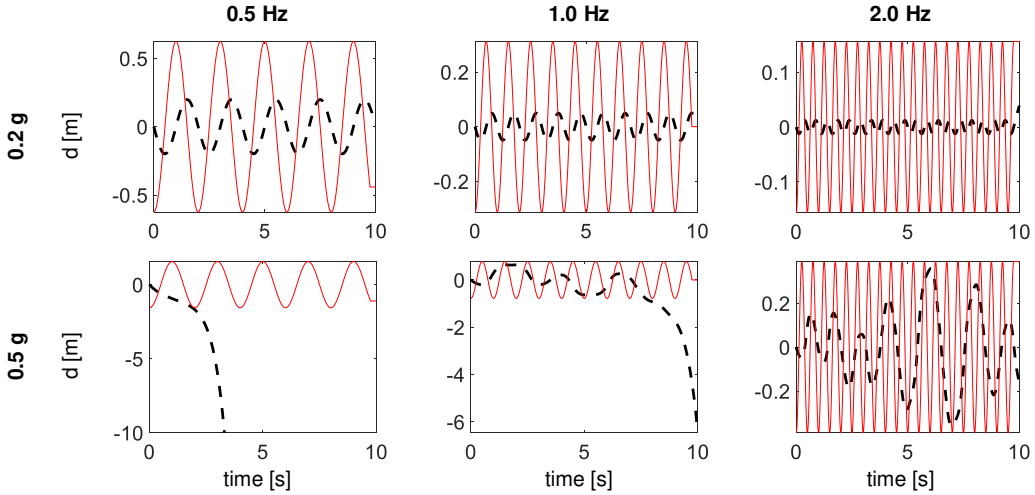

Figure 9: Base (red continuous line) and top (black dashed line) displacements for a moderately slender monolithic wall ($H/B = 4$) subjected to several harmonic excitations

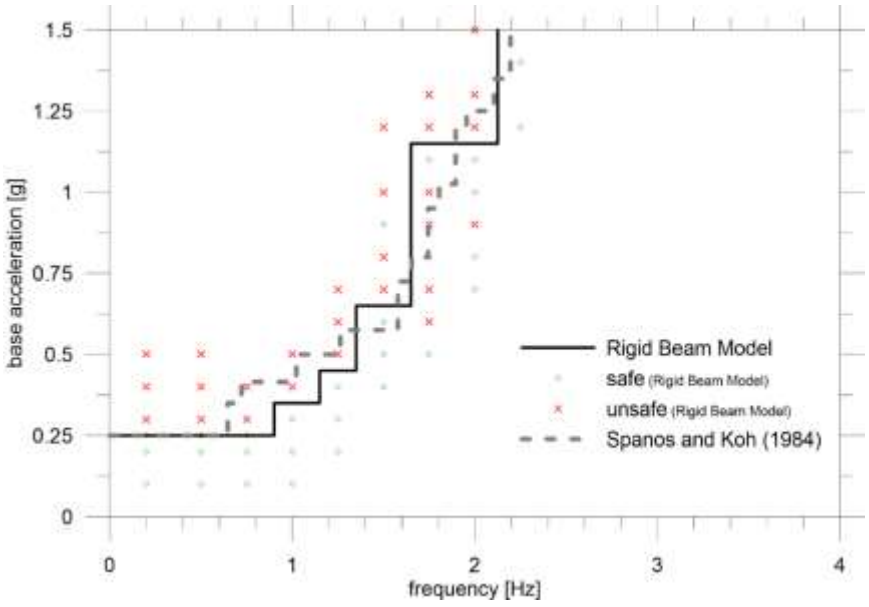

Figure 10: Safe-unsafe domain for a moderately slender monolithic wall ($H/B = 4$) subjected to harmonic excitations.

It is worth noting that the discrepancy with Spanos and Koh [**50**] work highlighted in Figure 7 is responsibility of the authors because the model is based on simplifications for the non-linear dynamic behavior made in such a way to linearize the displacements. As a consequence, if the wall/block is not slender, this implies errors that progressively increase. This aspect is evident by comparing Figure 7 with Figure 10, since in the latter one the fitting between the proposed and the existing models is very good.

3.1.3 Monolithic walls with increasing slenderness subjected to harmonic excitations

The case studies proposed in [**50**] are taken as preliminary reference for performing a parametric analysis on the effects of wall slenderness on the dynamic behavior of monolithic walls. For this purpose, starting from the geometric slenderness values H/B equal to 2 and 4 considered in the previous section, more slender monolithic walls having H/B equal to 8 and 12 are taken into consideration.
Figure 11a and b shows, respectively, the safe-unsafe domains obtained with the monolithic walls having H/B equal to 8 and 12. In both cases, collapse accelerations with input frequencies tending to zero are quite close to the static load multipliers of each load ($a_{g0} = (B/H)$ g); in the less slender case such initial value does not increase significantly for small frequency values, for instance up to 0.5 Hz and a similar behavior can be found with the thick and moderately slender walls considered previously. However, the collapse acceleration amplitudes for the two slender walls increase rapidly for input frequencies larger than 0.5 Hz; for instance, collapse accelerations close to 1g are obtained with 2 Hz with H/B equal to 8 and with 2.5 Hz if H/B is equal to 12.

Safe-unsafe domains are obviously depending on wall slenderness and, as can be expected, for a given value of input frequency, thick or moderately slender walls are characterized by an overturning acceleration larger than that typical of the slenderer walls. In order to appreciate the influence of wall slenderness on the collapse accelerations obtained for varying input frequency, Figure 12 a and b collects the safe-unsafe domains obtained with the four slenderness cases taken into consideration in this contribution. In particular, the dimensionless representation adopted in Figure 12 b allows to highlight a common behavior for the four slenderness cases considered.

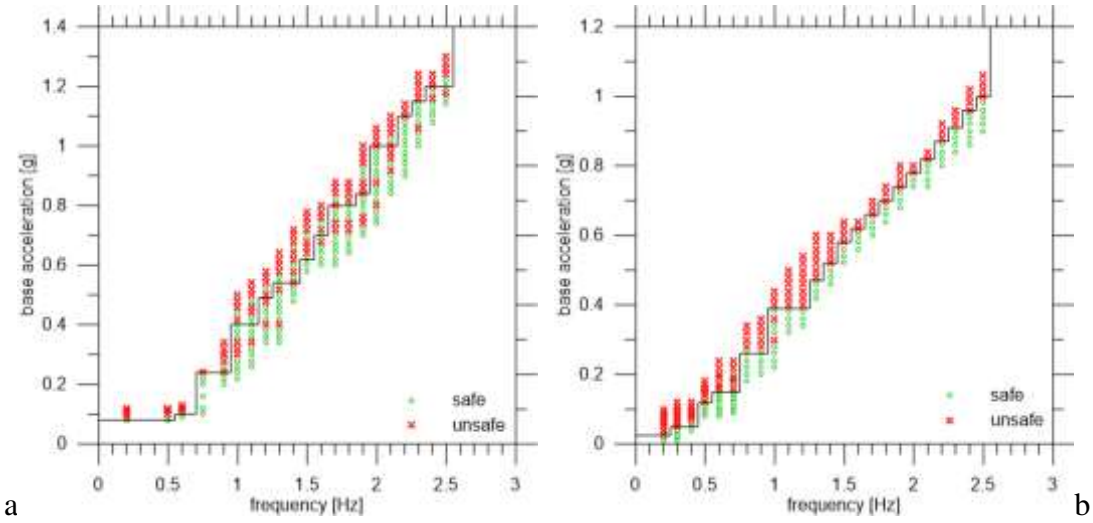

Figure 11: Safe-unsafe domains for two slender monolithic walls having H/B equal to 8 (a) and 12 (b) subjected to harmonic excitations.

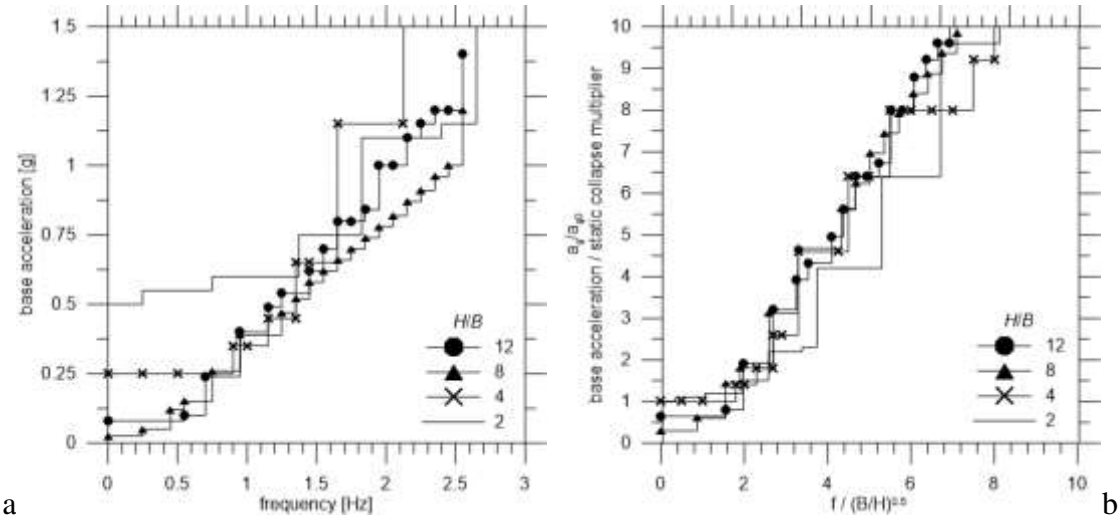

Figure 12: Safe-unsafe domains for monolithic walls having *H*/*B* equal to 2, 4, 8, and 12 subjected to harmonic excitations.

3.2 Multi-block walls

3.2.1 Influence of the number of wall portions on a moderately slender wall subjected to harmonic excitation

Starting from the numerical results obtained with the moderately slender wall ($H/B = 4$), which turned out to be in excellent agreement with the results by Spanos and Koh [**50**], here attention is devoted to the dynamic behavior of the multi-block walls equivalent to the monolithic ones. In particular, two and four equally spaced blocks or wall portions are considered and harmonic tests with varying input frequency and acceleration amplitude are performed.

Figure 13 a, b shows, respectively, the safe-unsafe domains obtained with *n* equal to 2 and 4. In both cases, the collapse acceleration obtained with frequencies tending to zero is close to the static collapse load multiplier of the monolithic wall, equal to $a_{g0} = (B/H)$ g = 025g. With two equally spaced blocks, the initial collapse accelerations do not increase significantly up to 1 Hz, then accelerations rapidly increase to 0.5g with 1.5 Hz. Considering the case having four equally spaced blocks, collapse accelerations start to decrease from 0.25g to 0.15g up to 1 Hz, then they increase rapidly to 0.5 g with 1.5 Hz.

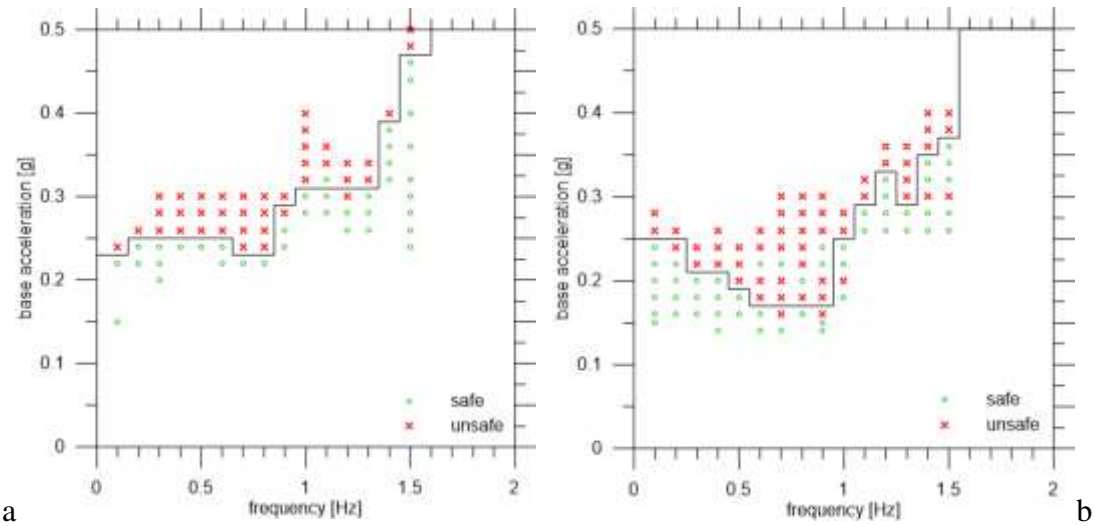

Figure 13: Safe-unsafe domains for monolithic walls having *H*/*B* equal to 4 and composed of 2 (a) and 4 (b) equally spaced blocks, subjected to harmonic excitations.

3.2.2 Slender hollow blocks concrete wall subjected to harmonic excitation

In order to show the effectiveness of the proposed rigid beam model in representing the dynamic behavior of a more realistic case study with respect to the cases considered in the previous sub-sections, a slender cantilever wall made of hollow concrete blocks is considered. The wall is made of hollow concrete blocks having length b = 0.60 m, thickness t = 0.40 m, and height a = 0.40 m. Ten blocks along the height of the wall are considered, hence an overall height H = 4 m and thickness B = 0.40 m are assumed for the wall, together with a unitary wall depth (Figure 14). Due to the plane strain hypothesis, the blocks arrangement in the in-plane direction of the wall is not taken into consideration, whereas the bed joints of the wall are assumed as interfaces of the rigid beam model corresponding to the wall, since such bed joints may represent potential cracks in case of a total or partial overturning of the wall. Wall density γ is equal to 1200 kg/m^3 and interface bending stiffness is defined by assuming an elastic modulus E = 2 GPa and interface thickness e = 0.01 m.

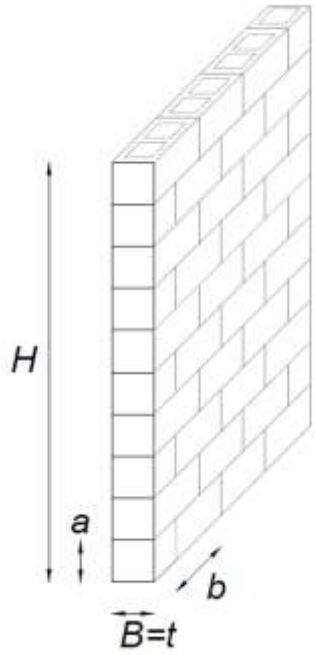

Figure 14: Slender multi-block wall composed of 10 hollow concrete blocks along its height.

Figure 15 collects several deformed configurations obtained at the end of the numerical tests or before the final collapse due to overturning of the wall or a wall portion. With an acceleration amplitude of 0.15 g, the wall collapses with 0.5 Hz showing an overturning mechanism involving the entire wall, and with 2.0 Hz, showing a mechanism involving a few blocks of the upper portion of the wall. With a harmonic excitation having frequency 1.0 Hz and amplitude 0.15 g, the wall turns out to remain in a safe condition, characterized by a small bending. On the other hand, three different overturning conditions are obtained with an acceleration equal to 0.25 g and varying input frequency; in particular, different wall portions are subjected to overturning in the three cases considered.

Figure 16 shows the safe-unsafe domain of the multi-block wall subjected to harmonic excitations with varying input frequency and acceleration magnitude. Collapse accelerations do not increase monotonically for increasing input frequency, but they are characterized by several increasing-decreasing phases up to 7 Hz. In particular, for very small frequency values, collapse accelerations increase from 0.04g to 0.2g up to 1.5 Hz, then they decrease to 0.1g with 2.5 Hz. A second increasing phase to 0.36 g is observed up to 5 Hz, whereas a reduction of collapse acceleration values to 0.3 Hz

is found at 6 and 7 Hz. Finally, for frequency values larger than 7 Hz, collapse accelerations rapidly increase to 0.6 g with 10 Hz.

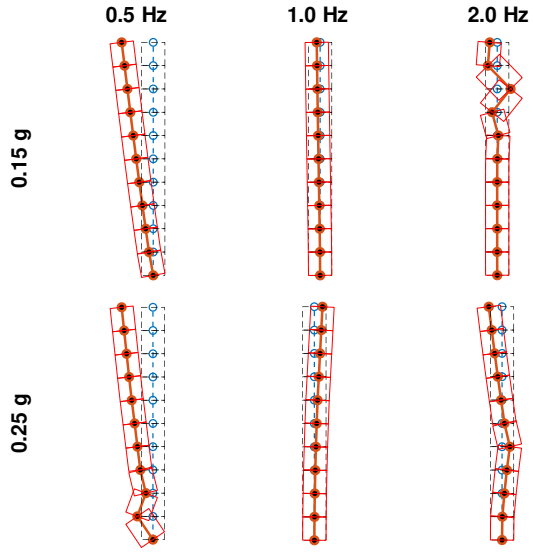

Figure 15: Deformed configurations for a slender multi-block concrete wall having H = 4 m B = 0.4 m and composed by 10 hollow concrete blocks along its height.

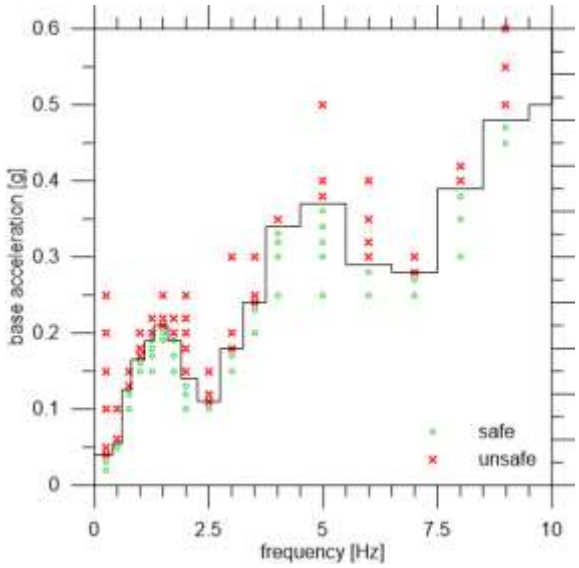

Figure 16: Safe-unsafe domain for a multi-block concrete wall having H = 4 m B = 0.4 m and composed by 10 hollow concrete blocks along its height.

3.2.3 Sensitivity analyses on hollow blocks concrete walls

In order to highlight the influence of the main geometric parameters of the slender wall considered in the previous sub-section on its dynamic behavior and the corresponding collapse mechanisms for varying input frequency, a set of sensitivity analyses is performed by varying wall thickness B and block height h, keeping fixed wall overall height H. In particular, on one hand, wall thickness B is varied from 0.40 m to 0.60 m and 0.80 m keeping fixed block and wall height h = 0.4 m and H = 4 m; on the other hand, h is varied from 0.4 m to 0.8 m and 2.0 m keeping fixed wall thickness and height B = 0.4 m and H = 4 m, leading to walls made of n equal to 5 and 2 portions, respectively.

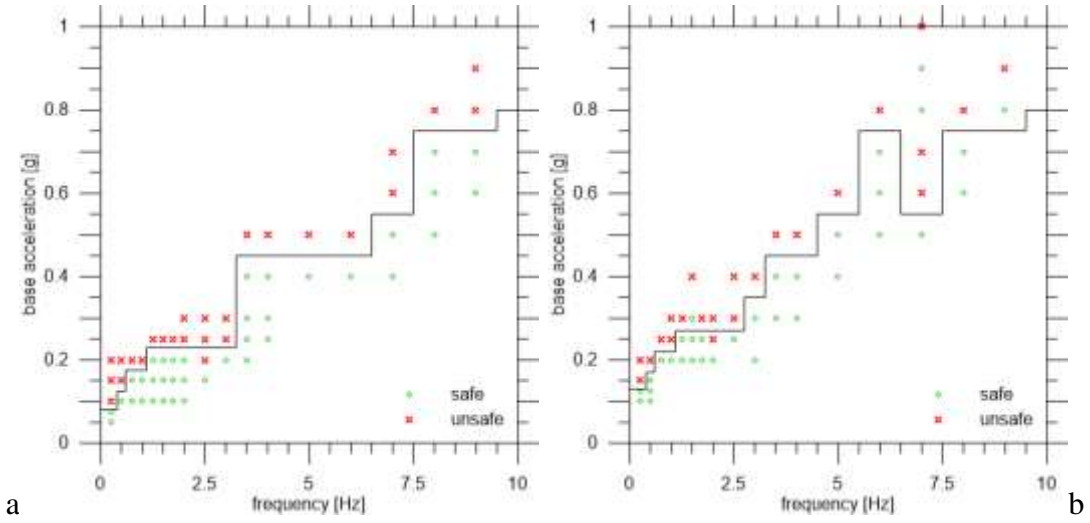

Figure 17: Safe-unsafe domain for a multi-block concrete wall having $H = 4$ m, composed by 10 hollow concrete blocks along its height and having thickness $B = 0.60$ m (a) and $B = 0.80$ m (b).

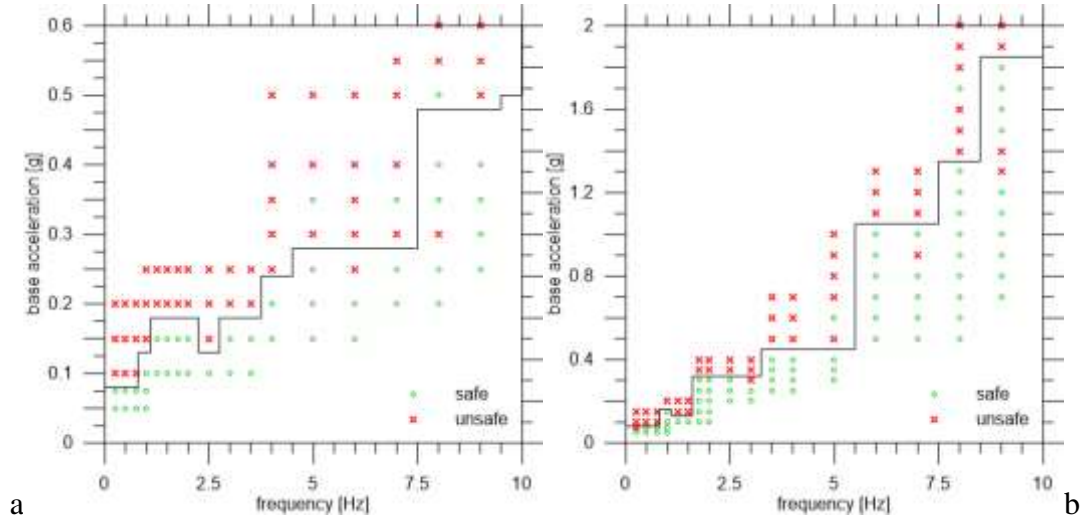

Figure 18: Safe-unsafe domain for a multi-block wall having $H = 4$ m $B = 0.4$ m, composed by 5 (a) and 2 (b) portions along its height.

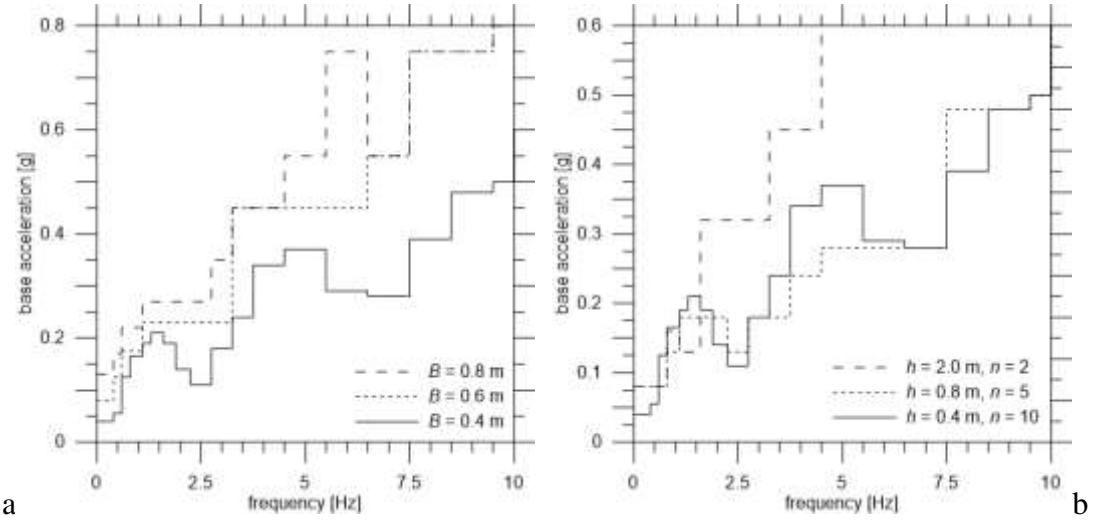

Figure 19: Safe-unsafe domains for a multi-block wall with varying several geometric parameters.

Figure 17 a and b collects safe-unsafe domains obtained with B = 0.6 and 0.8 m, respectively, which are compared to the domain obtained in the previous sub-section in Figure 19a. Figure 18 a and b collects safe-unsafe domains obtained with h = 0.8 and 2.0 m, respectively, which are compared to the domain obtained in the previous sub-section in Figure 19b.

In the first case, the influence of the wall and block thickness is quite significan the safe-unsafe domain of the walls with respect to the original one, this is justified by the slenderness variation of the proposed cases (H/B = 0.67 and 5.0 with B = 0.6 m and 0.8 m, respectively) with respect to the original one (H/B = 10).

In the second case, the height of wall portions, which is related to the number of rigid beam elements of the model, plays an important role only if a small number of portions is adopted. The case characterized by portion height h = 0.8 m has a safe-unsafe domain very close to that of the original wall, whereas the case having h = 2.0 m leads to a completely different safe-unsafe domain, with larger acceleration amplitudes with respect to those obtained with the original case.

Several collapse mechanisms obtained with frequencies increasing from 0.5 Hz to 8 Hz are collected in Figure 20. It is clear that collapse mechanisms obtained with small frequency values are characterized by the overturning of the entire panel, whereas for increasing input frequency, the collapse mechanisms are characterized by the subdivision of the wall into 2-3 portions, with the upper ones rocking with respect to each other and the base one remaining fixed. This aspect is also evident if the h increases and, consequently, the number of subdivisions n along wall height is reduced from 10 to 5 and 2, since overturning mechanisms for the entire wall are obtained with small frequency values, whereas the relative rotations of wall portions with respect to each other are obtained for increasing frequency.

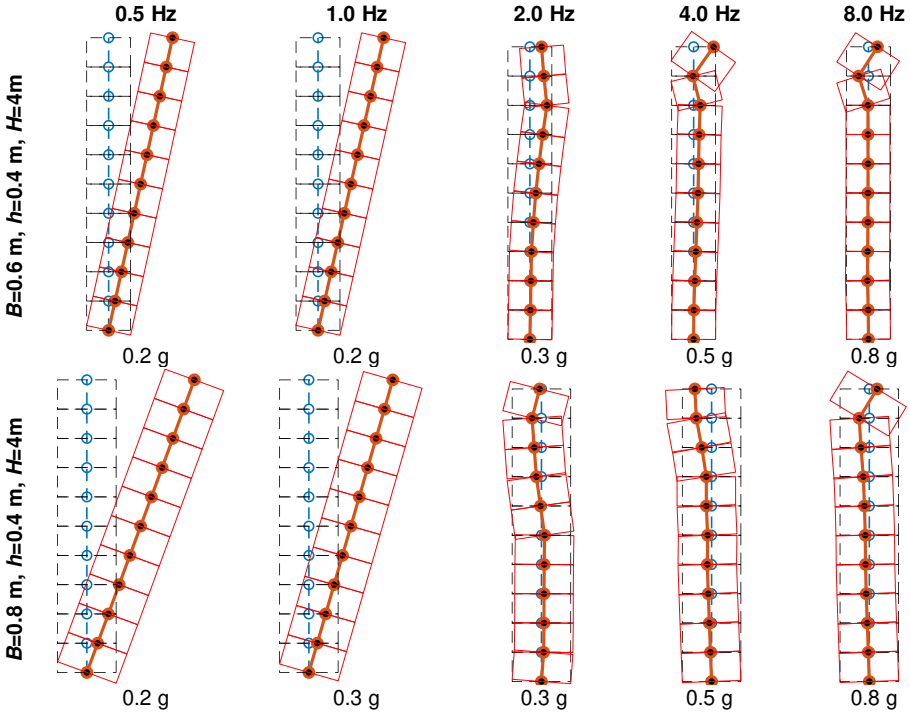

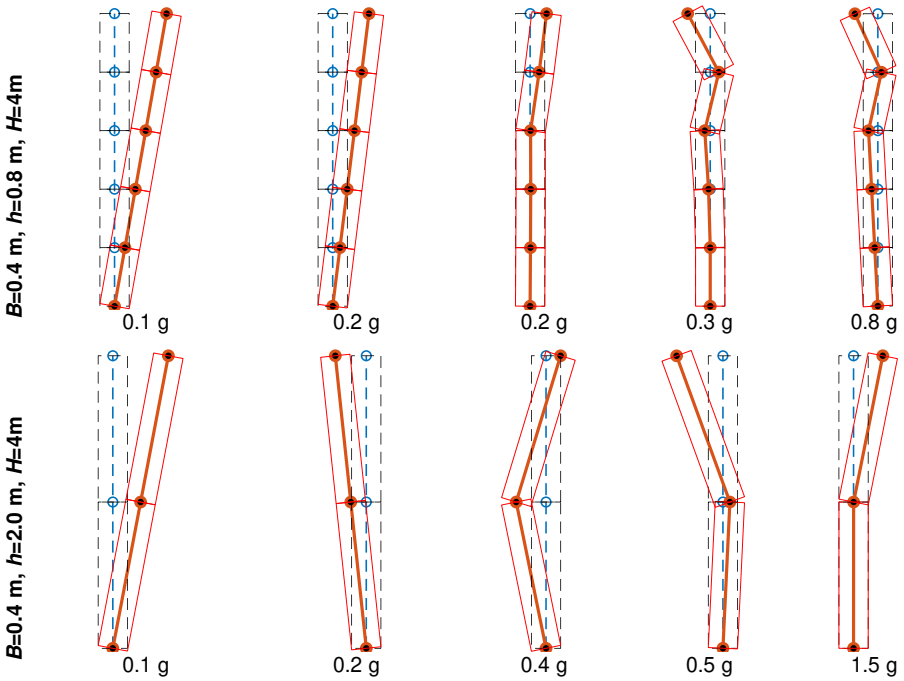

Figure 20: Deformed configurations and corresponding collapse accelerations for a slender multi-block wall with varying several geometric parameters.

4 CONCLUSIONS AND FURTHER DEVELOPMENTS

In this contribution, a simple and effective rigid beam model, recently introduced by authors for studying the dynamic behavior of freestanding monolithic and multi-drum columns, is extended to the analysis of cantilever unreinforced masonry walls subjected to out-of-plane dynamic actions.
The model is introduced for representing out-of-plane loaded walls in plane state, hence by considering their transversal section along the wall thickness, whereas the blocks arrangement along wall depth is not taken into consideration. Monolithic and multi-block walls are investigated, in the latter case by subdividing the wall section into equal portions in vertical direction which may represent on one hand actual stone, clay or concrete blocks connected by mortar joints, on the other hand they can represent portions of wall made of irregular stones, where the interfaces may represent potential horizontal cracks.

The proposed rigid beam model assumes each block or wall portion as a rigid beam element and each interface as a node of the model. By assuming small displacements and no sliding at the interfaces, potential rocking between the blocks is taken into account by assuming a bi- or tri-linear moment-rotation nonlinear constitutive law.

Harmonic tests on monolithic and multi-block cantilever walls are performed by varying input frequency and acceleration magnitude, and by considering several case studies having different wall slenderness. The proposed model turned out to be in very good agreement with some of the existing numerical results assumed as reference **[50]**. Furthermore, a set of parametric tests dedicated to the influence of wall slenderness on the dynamic behavior of monolithic walls, together with the assessment of the harmonic response of a multi-block wall made of hollow concrete blocks, allowed to highlight the effectiveness of the model and its applicability to a wide range of case studies.

Numerical results showed, as expected, that monolithic walls can overturn with acceleration magnitudes larger than their corresponding static load multipliers if input frequency values increase.

However, overturning accelerations of multi-block walls increase less rapidly for increasing input frequency with respect to the corresponding equivalent monolithic walls.

Numerical tests performed on a more realistic slender wall composed of ten hollow concrete blocks along its height allowed to better highlight the capability of the rigid beam model in activating non-standard failure mechanisms, such as the overturning of an upper portion of the wall or the formation of two plastic hinges along wall height. This behavior has been confirmed by a subsequent sensitivity analysis with varying wall thickness and block height and keeping fixed wall height. Collapse mechanism generally turned out to be overturning ones of the entire wall with respect to its base only with small input frequency values, with collapse acceleration values very close to the static load multipliers of the corresponding walls. Increasing input frequency,

Thanks to the simple and effective matrix representation of the system of equations of motion adopted for the model, further developments of the current version of the rigid beam model will be taken into consideration. On one hand, more complex boundary conditions for the wall, namely a wall with fixed or pinned base and also pinned at the top for representing the effect of a roof or an intermediate slab, will be investigated, in order to numerically simulate the huge set of laboratory dynamic tests performed up to recent years by many authors **[34-41]**. On the other hand, the mass, geometric and polar inertia matrices will be better detailed in order to simulate more realistic case studies of masonry walls subjected to additional vertical loads and made of blocks having different size along wall height.

REFERENCES

[1] Bruneau, M. (1994). State-Of-The-Art Report On Seismic Performance Of Unreinforced Masonry Buildings, American Society of Civil Engineers – Journal of the Structural Division, 120(1):230-251.

[2] Decanini, L. D., Gavarini, C. & Mollaioli, F. (2000). Some remarks on the Umbria-Marche earthquakes of 1997. European Earthquake Engineering, 14(3): 18-48.

[3] Decanini L., De Sortis A., Goretti A., Langenbach R., Mollaioli F. & Rasulo A. (2004). Performance of masonry buildings during the 2002 Molise, Italy, Earthquake. Earthquake Spectra, July 2004, 20(S1): S191-S220.

[4] Augenti N., Parisi F., Learning from Construction Failures due to the 2009 L'Aquila, Italy, Earthquake, Journal of Performance of Constructed Facilities (2010) 24(6) 536-555.

[5] D'Ayala D., Paganoni S., Assessment and analysis of damage in L'Aquila historic city centre after 6th April 2009, Bulletin of Earthquake Engineering (2011) 9(1) 81-104.

[6] Ingham, J. M., Biggs, D. T. & Moon, L. M. (2011). How did unreinforced masonry buildings perform in the February 2011 Christchurch earthquake? The Structural Engineer, 89(6), 14-18.

[7] Penna, A., Morandi, P., Rota, M., Manzini, C.F., da Porto, F., Magenes, G. Performance of masonry buildings during the Emilia 2012 earthquake (2014) Bulletin of Earthquake Engineering, 12 (5), pp. 2255-2273.

[8] Gabriele Fiorentino, Angelo Forte, Enrico Pagano, Fabio Sabetta, Carlo Baggio, Davide Lavorato, Camillo Nuti & Silvia Santini, Damage patterns in the town of Amatrice after August 24th 2016 Central Italy earthquakes, Bulletin of Earthquake Engineering volume 16, pages1399–1423(2018).

[9] Ferreira TM, Costa AA, Costa A. Analysis of the out-of-plane seismic behavior of unreinforced masonry: a literature review. Int. J. Architect. Heritage 2015;9(8):949–72.

[10] L. Sorrentino, D. D'Ayala, G. Felice, MC Griffith, S. Lagomarsino, G. Magenes. Review of out-of-plane seismic assessment techniques applied to existing masonry buildings. Int J Archit Heritage. 2016;11(1):2-21.

[11] D'Altri, A. M., Sarhosis, V., Milani, G., Rots, J., Cattari, S., Lagomarsino, S., . . . de Miranda, S. (2020). Modeling strategies for the computational analysis of unreinforced masonry structures: Review and classification. Archives of Computational Methods in Engineering, 27(4), 1153-1185.

[12] Zhang X, Singh S, Bull DK, Cooke N. Out-of-plane performance of reinforced masonry walls with openings. J Struct Eng 2001;127(1):51–7.

[13] Milani G, Lourenço P, Tralli A. Homogenization approach for the limit analysis of out-of-plane loaded masonry walls. J Struct Eng 2006;132(10):1650–63.

[14] Cecchi A, Milani G, Tralli A. A Reissner-Mindlin limit analysis model for out-of plane loaded running bond masonry walls. International journal of solids and structures 2007;44(5):1438–60.

[15] Milani G, Lourenço PB. A simplified homogenized limit analysis model for randomly assembled blocks out-of-plane loaded. Comput Struct 2010;88(11–12):690–717.

[16] Varela-Rivera JL, Navarrete-Macias D, Fernandez-Baqueiro LE, Moreno EI. Out-of plane behaviour of confined masonry walls. Eng Struct 2011;33(5):1734–41.

[17] Milani G. Simple lower bound limit analysis homogenization model for in-and out-of-plane loaded masonry walls. Constr Build Mater 2011;25(12):4426–43.

[18] Milani G, Tralli A. Simple SQP approach for out-of-plane loaded homogenized brickwork panels accounting for softening. Comput Struct 2011;89(1–2):201–15.

[19] Casolo S, Milani G. Simplified out-of-plane modelling of three-leaf masonry walls accounting for the material texture. Constr Build Mater 2013;40:330–51.

[20] Agnihotri P, Singhal V, Rai DC. Effect of in-plane damage on out-of-plane strength of unreinforced masonry walls. Eng Struct 2013;57:1–11.

[21] Milani G, Pizzolato M, Tralli A. Simple numerical model with second order effects for out-of-plane loaded masonry walls. Eng Struct 2013;48:98–120.

[22] Kevin Q. Walsh, Dmytro Y. Dizhur, Jalil Shafaei, Hossein Derakhshan, Jason M. Ingham, In Situ Out-of-Plane Testing of Unreinforced Masonry Cavity Walls in as-Built and Improved Conditions, Structures, Volume 3, 2015, Pages 187-199,

[23] Silva LC, Lourenço PB, Milani G. Nonlinear discrete homogenized model for out-of-plane loaded masonry walls. J Struct Eng 2017;143(9):04017099.

[24] Asteris PG, Cavaleri L, Di Trapani F, Tsaris AK. Numerical modelling of out-of-plane response of infilled frames: State of the art and future challenges for the equivalent strutmacromodels. Eng Struct 2017;132:110–22.

[25] Ridwan M, Yoshitake I, Nassif AY. Two-dimensional fictitious truss method for estimation of out-of-plane strength of masonry walls. Constr Build Mater 2017;152:24–38.

[26] Sorrentino L, D'Ayala D, de Felice G, Griffith MC, Lagomarsino S, Magenes G. Review of out-of-plane seismic assessment techniques applied to existing masonry buildings. Int J Architectural Heritage 2017;11(1):2–21.

[27] Silva LC, Lourenço PB, Milani G. Derivation of the out-of-plane behaviour of masonry through homogenization strategies: Micro-scale level. Comput Struct 2018;209:30–43.

[28] H. Derakhshan, W. Lucas, P. Visintin, M.C. Griffith, Out-of-plane Strength of Existing Two-way Spanning Solid and Cavity Unreinforced Masonry Walls, Structures, Volume 13, 2018, Pages 88-101,

[29] Kevin Walsh, Dmytro Dizhur, Ivan Giongo, Hossein Derakhshan, Jason Ingham, Predicted Versus Experimental Out-of-plane Force-displacement Behaviour of Unreinforced Masonry Walls, Structures, Volume 15, 2018, Pages 292-306.

[30] Lang-Zi Chang, Francesco Messali, Rita Esposito, Capacity of unreinforced masonry walls in out-of-plane two-way bending: A review of analytical formulations, Structures, Volume 28, 2020, Pages 2431-2447.

[31] Malomo D, Pinho R, Penna A. Numerical modelling of the out-of-plane response of full-scale brick masonry prototypes subjected to incremental dynamic shake-table tests. Eng Struct 2020;209:110298.

[32] Noor-E-Khuda S, Dhanasekar M. On the out-of-plane flexural design of reinforced masonry walls. J Building Eng 2020;27:100945.

[33] Pirsaheb, H., Javad Moradi, M., & Milani, G. (2020). A multi-pier MP method for the non-linear static analysis of out-of-plane loaded masonry walls. Engineering Structures, 223.

[34] P. Gulkan, R. Clough, R. Mayes and G. Manos. Seismic testing of single-story masonry houses: part 1 and 2. Journal of Structural Engineering (1990), 116: 235-274.

[35] Lam, N. T. K., J. L. Wilson, and G. L. Hutchinson. The seismic resistance of unreinforced masonry cantilever walls in low seismicity areas. Bull. N. Z. Nat. Soc. Earthquake Eng., 1995; 28 (3): 179–195.

[36] Doherty, K. 2000. "An investigation of the weak links in the seismic load path of unreinforced masonry building." Ph.D. thesis, Dept. of Civil and Environmental Engineering, Univ. of Adelaide.

[37] M.C Griffith., N.T.K. Lam, Wilson J.L., Doherty K., Experimental Investigation of Unreinforced Brick Masonry Walls in Flexure. J. Struct. Eng., 2004, 130(3): 423-432.

[38] C. Simsir, M. Aschheim and D. Abrams. Out of plane dynamic response of unreinforced masonry bearing walls attached to flexible diaphragms. In Proceedings of the 13th World Conference on Earthquake Engineering, Vancouver, B.C., 1-4 August 2004. International Association for Earthquake Engineering, Tokyo, Japan.

[39] C.C. Simsir, M.A. Aschheim, D.P. Abrams, Out-of-plane dynamic response of unreinforced masonry bearing walls attached to flexible diaphragms. 13th World Conference on Earthquake Engineering, Vancouver, B.C., Canada, August 1-6, 2004, Paper No. 2045.

[40] Giaretton, M., D. Dizhur, and J. M. Ingham. Dynamic testing of as-built clay brick unreinforced masonry parapets. 2016; Eng. Struct. 127 (Nov): 676–685

[41] Graziotti, F., U. Tomassetti, A. Penna, and G. Magenes. Out-of plane shaking table tests on URM cavity walls. Eng. Struct. 2016; 125 (Oct): 455–470.

[42] E.D. Erwing, A.W. Johnson and J.C. Kariotis. Methodology for mitigation of seismic hazards in existing unreinforced masonry buildings: wall testing, out of plane. (1981). El Segundo, Calif ABK Topical Report 04.

[43] Milne J (1881) Experiments in observational seismology. Trans Seismol Soc Japan 3:12-64.

[44] Omori F (1900) Seismic experiments on the fracturing and overturning of columns. Bulletin of the Imperial Earthquake Investigation Committee 4(1):1-31

[45] Housner GW (1963) The behavior of inverted pendulum structures during earthquakes. Bulletin of Seismological Society of America, 53(1), 403-417.

[46] Aslam M, Godden WG, Scalise DT (1980) Earthquake rocking response of rigid bodies. J Eng Mech Div ASCE 106(2):377-392.

[47] Yim CS, Chopra AK, Penzien J (1980) Rocking response of rigid blocks to earthquakes. Earthquake Eng Struct Dyn 8:565-587.

[48] Ishiyama Y (1982) Motions of rigid bodies and criteria for overturning by earthquake excitations. Earthquake Eng Struct Dyn 10:635-650.

[49] Psycharis IN, Jennings PC (1983) Rocking of slender rigid bodies allowed to uplift. Earthquake Eng Struct Dyn 11:57-76.

[50] Spanos PD, Koh AS (1984) Rocking of rigid blocks due to harmonic shaking. J Eng Mech 110(11):1627-1642.

[51] Sinopoli A (1987) Dynamics and impact in a system with unilateral constraints the relevance of dry friction. Meccanica 22:210-215.

[52] Tso WK, Wong CM. Steady state rocking response of rigid blocks part 1: Analysis. Earthq Eng Struct Dyn 1989;18(1):89–106.

[53] Augusti G, Sinopoli A. Modelling the dynamics of large block structures. Meccanica 1992;27:195–211.

[54] Andreaus U, Casini P. Rocking-sliding of a rigid block: friction influence on free motion. Eng Trans 1998;46(2):143–64.

[55] Lenci S, Rega G. A dynamical systems approach to the overturning of rocking blocks. Chaos Solitons Fractals 2006;28:527–42

[56] Sorrentino, L., Masiani, R. & Decanini, L. D. (2006a). Overturning of rocking rigid bodies under transient ground motions. Structural Engineering and Mechanics, 22(3): 293-310.

[57] Pena F, Prieto F, Lourenço PB, Costa AC, Lemos JV. On the dynamics of rocking motion of single rigid-block structures. Earthq Eng Struct Dyn 2007;36(15):2383–99.

[58] O. Al Shawa, G. de Felice, A. Mauro and L. Sorrentino, Out-of-plane seismic behaviour of rocking masonry walls, Earthquake Engng Struct. Dyn. 2012; 41:949–968

[59] S. J. Hogan, On the dynamics of rigid-block motion under harmonic forcing, Proc. R. Soc. London, A425, 441-476, (1989).

[60] Hogan SJ, The many steady state responses of a rigid block under harmonic forcing, Earthquake ENG. AND STR. DYNAMICS, VOL. 19, 1057-1071, (1990).

[61] K. Doherty, M. C. Griffith, N. Lam and J. Wilson; Displacement-based seismic analysis for out-of-plane bending of unreinforced masonry walls; Earthq Eng Struct Dyn 2002; 31:833–850.

[62] N.T.K. Lam, M. Griffith, J. Wilson, K. Doherty. Time–history analysis of URM walls in out-of-plane flexure, Eng. Struct., 25 (2003) 743–754.

[63] M.C. Griffith; N.T.K. Lam; J.L. Wilson; and K. Doherty 2004. Experimental Investigation of Unreinforced Brick Masonry Walls in Flexure. Journal of Structural Engineering, 130(3):423-432.

[64] H. Derakhshan, J.M. Ingham, M.C. Griffith; Out-of-Plane Assessment of an Unreinforced Masonry Wall: Comparison with NZSEE Recommendations; 2009 NZSEE Conference; paper no. 33.

[65] L. Sorrentino, R. Masiani, L.D. Decanini; Overturning of rocking rigid bodies under transient ground motions; Struct Eng Mech 3006; 22(3):293-310.

[66] Psycharis IN. Dynamic behaviour of rocking two-block assemblies. Earthq Eng Struct Dyn 1990;19:555–75

[67] Sinopoli A. Dynamic analysis of a stone column excited by a sine wave ground motion. Appl Mech Rev 1991;44(11):S246–55.

[68] Spanos PD, Roussis PC, Politis NPA. Dynamic analysis of stacked rigid blocks. Soil Dyn Earthq Eng 2001;21:559–78.

[69] Kounadis AN, Papadopoulos GJ. On the rocking instability of 3-rigid block system under ground excitation. Arch Appl Mech 2016;86:957–77.

[70] Kounadis AN. The effect of sliding on the rocking instability of multi-ridgid block assemblies under ground motion. Soil Dyn Earthq Eng 2018;104:1–14.

[71] Azevedo J, Sincrain G, Lemos JV. Seismic behavior of blocky masonry structures. Earthquake Spectra 2000; 16(2):337–365.

[72] Hori N, Inoue N, Purushotam D, Nishida T, Kobayashi J. Experimental and analytical studies on earthquake resisting behaviour of confined concrete block masonry structures. Earthquake Engineering and Structural Dynamics 2006; 35:1699–1719. DOI: 10.1002/eqe.604.

[73] NTUA. Monuments under seismic action. A numerical and experimental approach. Report No. NTUA/LEE-97/01, Laboratory for Earthquake Engineering, Faculty of Civil Engineering, National Technical University of Athens, 1997.

[74] Papantonopoulos C, Psycharis N, Papastamatiou DY, Lemos JV, Mouzakis HP. Numerical prediction of the earthquake response of classical columns using the distinct element method. Earthquake Engineering and Structural Dynamics 2002; 31:1699–1717. DOI: 10.1002/eqe.185.

[75] Psycharis N, Lemos JV, Papastamatiou DY, Zambas C, Papantonopolous C. Numerical study of the seismic behaviour of a part of the Parthenon Pronaos. Earthquake Engineering and Structural Dynamics 2003; 32: 2063–2084. DOI: 10.1002/eqe.315.

[76] Winkler T, Meguro K, Yamazaki F. Response of rigid body assemblies to dynamic excitation. Earthquake Engineering and Structural Dynamics 1995; 24:1389–1408.

[77] Dimitri R, De Lorenzis L, Zavarise G. Numerical study on the dynamic behavior of masonry columns and arches on buttresses with the discrete element method. Eng Struct 2011;33:3172–88.

[78] Pulatsu B, Sarhosis V, Bretas E, Nikitas N, Lourenço PB. Non-linear static behaviour of ancient free-standing stone columns. Struct Build 2017:1–13. [2017, (ePub ahead of Print].

[79] Sarhosis V, Asteris P, Wang T, Hu W, Han Y. On the stability of colonnade structural systems under static and dynamic loading conditions. Bull Earthq Eng 2016;14(4):1131–52. [2016].

[80] Sarhosis, V., Baraldi, D., Lemos, J. V., & Milani, G. (2019). Dynamic behaviour of ancient freestanding multi-drum and monolithic columns subjected to horizontal and vertical excitations. Soil Dynamics and Earthquake Engineering, 120, 39-57.

[81] Bora Pulatsu, Ece Erdogmus, Paulo B. Lourenço, Jose V. Lemos, Kagan Tuncay, Simulation of the in-plane structural behavior of unreinforced masonry walls and buildings using DEM, Structures, Volume 27, 2020, Pages 2274-2287.

[82] D. D'Ayala, Y. Shi; Modeling Masonry Historic Buildings by Multi-Body Dynamics; Int J Archi Herit 2011; 5:483–512.

[83] C. Casapulla, L. Giresini, P.B. Lourenço; Rocking and Kinematic Approaches for Rigid Block Analysis of Masonry Walls: State of the Art and Recent Developments; Buildings 2017, 7,69,1-19.

[84] ASCE 2007. Seismic rehabilitation of existing buildings. Standard ASCE/SEI 41-06. American Society of Civil Engineers, Reston, Va.

[85] CNTC2009. Circolare 02/02/2009 n. 617. Istruzioni per l'applicazione delle Nuove norme tecniche per le costruzioni di cui al Decreteo, Ministeriale 14/1/2008. Gazzetta Ufficiale della Repubblica Italiana n. 47, Supplemento Ordinario n. 27 (in Italian).

[86] NTC 2008. Decreto Ministeriale 14/1/2008. Nuove norme tecniche per le costruzioni. Ministry of Infrastructures and Transportations. Gazzetta Ufficiale della Repubblica Italiana n. 29, Supplemento Ordinario n. 30 (in Italian).

[87] M. Godio & K. Beyer Evaluation of force-based and displacement-based out-of-plane seismic assessment methods for unreinforced masonry walls through refined model simulations, Earthquake Engineering Structural Dynamics. 2018; 48:454–475.

[88] Itasca. UDEC - Universal Distinct Element Code manual: theory and background. Minneapolis, Itasca Consulting Group, (2004).

[89] P.A. Cundall, A computer model for simulating progressive large scale movements in blocky rock systems. Proceedings of the Symposium of the International Society of Rock Mechanics (1971), Nancy, France.

[90] M. Godio & K. Beyer Trilinear Model for the Out-of-Plane Seismic Assessment of Vertically Spanning Unreinforced Masonry Walls, 2019, Journal of Structural Engineering 145(12):1-13.

[91] D. Baraldi, G. Milani, and V. Sarhosis, Numerical models for simulating the dynamic behaviour of freestanding ancient columns. Compdyn 2019 Proceedings (2019), pages 1526-1536.

[92] Rondelet, J. Traité théorique et pratique de l'art du batir, 1802; Vol. 5. Paris, France: Chez l'Auteur.

[93] C.S. Meisl, K.J. Elwood, C.E. Ventura, Shake table tests on the out-of-plane response of unreinforced masonry walls. Can. J. Civ. Eng. 34: 1381-1392 (2007).

[94] F. Graziotti, U. Tomassetti, A. Penna, G. Magenes. Out-of-plane shaking table tests on URM single leaf and cavity walls, Engineering Structures 125 (2016) 455–470.

[95] O. Penner, K.J. Elwood, Out-of-Plane Dynamic Stability of Unreinforced Masonry Walls in One-Way Bending: Shake Table Testing. Earthquake Spectra, Volume 32, No. 3, pages 1675–1697, 2016.